

Improving the Initiation Efficiency in the Single Electron Transfer Living Radical Polymerization of Methyl Acrylate with Electronic Chain-End Mimics

NGA H. NGUYEN, BRAD M. ROSEN, VIRGIL PERCEC

Roy and Diana Vagelos Laboratories, Department of Chemistry, University of Pennsylvania, Philadelphia, Pennsylvania 19104-6323

Received 18 November 2010; accepted 6 December 2010

DOI: 10.1002/pola.24543

Published online 3 January 2011 in Wiley Online Library (wileyonlinelibrary.com).

ABSTRACT: Computational studies on the heterolytic bond dissociation energies and electron affinities of methyl 2-bromopropionate (MBP) and ethyl 2-bromoisobutyrate (EBiB) in the dissociative electron transfer (DET) step of single electron transfer living radical polymerization (SET-LRP) of methyl acrylate (MA) combined with kinetic experiments were performed in an effort to design the most efficient initiation system. This study suggests that EBiB is more effective than MBP in the SET-LRP of acrylates catalyzed by Cu(0) wire, thus being a true electronic mimic of the dormant PMA species. EBiB allows for a more predictable dependence of the molecular weight evolution and distribution. This is exemplified by the absence of a deviation in the PMA molecular weight from theoretical values at low conversions, as a result of a faster SET activation with

EBiB than with MBP. The enhanced control over molecular weight evolution was also observed in the SET-LRP of MA initiated with bifunctional initiators similar in structure to MBP and EBiB, suggesting a higher reactivity than MBP in the SET activation, which matches closely that of the polymer dormant chains. The use of bifunctional initiators in conjunction with activated Cu(0) wire in SET-LRP allows for dramatically accelerated polymerizations, although still providing for exceptional control of the molecular weight evolution and distribution. © 2011 Wiley Periodicals, Inc. *J Polym Sci Part A: Polym Chem* 49: 1235–1247, 2011

KEYWORDS: initiator; kinetics (polym.); methyl acrylate; radical polymerization; SET-LRP

INTRODUCTION The precise synthesis of polymers with well-defined compositions, architectures, and perfect structural fidelity has been of great interest in the field of polymer chemistry.¹ Considered as one of the most rapidly developing areas in polymer science, metal-catalyzed living radical polymerization (LRP) has provided synthetic polymer chemists with methods and strategies that can compete with organic reactions in the preparation of complex macromolecular structures otherwise inaccessible with conventional polymerization methods.^{2,3}

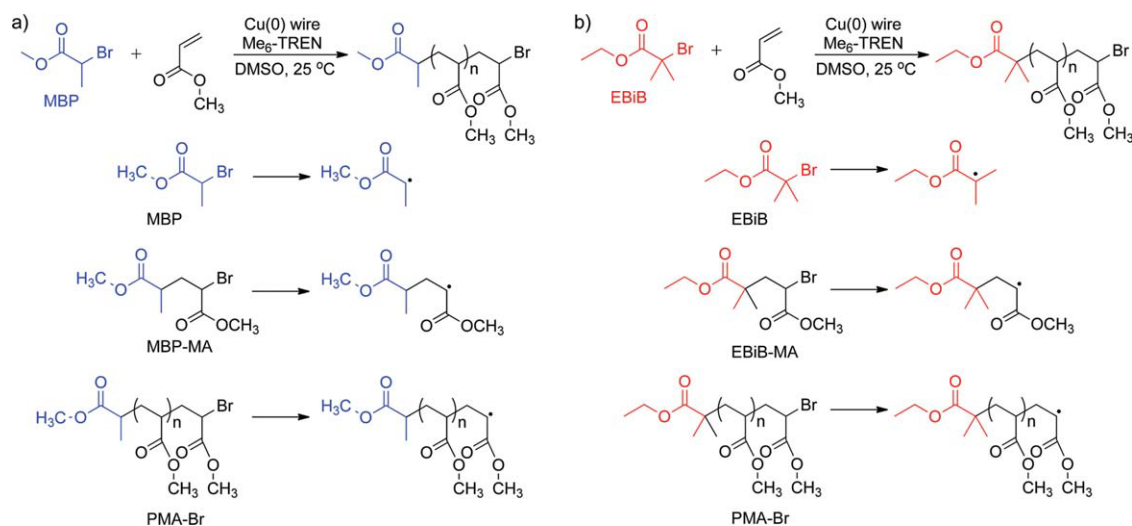
Single electron transfer LRP (SET-LRP)^{1,4} is emerging as a powerful tool for the rapid polymerization of functional acrylates,^{5–7} acrylamides,⁶ methacrylates,^{4,8–12} and vinyl chloride,^{4,13,14} with excellent control over the molecular weight evolution and distribution. It allows the precise synthesis of a range of polymeric structures, for example, dendritic macromolecules,^{2,15} star polymers,¹⁶ telechelic functional polymers,¹⁷ and graft copolymers.^{7,18} Mechanistically, the activation step in SET-LRP involves a heterolytic bond cleavage of the carbon–halide bond via a heterogeneous Cu(0)-catalyzed outer-sphere SET process.^{1,4,19,20} The ligand/solvent mediated-disproportionation of the *in situ* generated

Cu(I)X establishes the proper equilibrium between the active and dormant chains, which in turn enables an effective SET-LRP.^{1,4}

As with all metal-catalyzed LRP processes, the appropriate choice of initiator is critical. Rapid and quantitative initiation is required to achieve well-defined polymers with narrow molecular weight distributions. Nevertheless, if initiation is too fast, increased bimolecular termination of propagating radicals would result.²¹ Therefore, the initiator reactivity should be matched to the monomer reactivity. One strategy is to employ initiator molecules that structurally mimic the propagating dormant macroradicals.^{21,22} 2-Halopropionates such as methyl 2-bromopropionate (MBP) are among the most commonly used monofunctional initiators for metal-catalyzed LRP, including SET-LRP, of acrylates because of their structural resemblance to the monomers.^{1,23} A variety of 2-bromopropionate derivatives including bifunctional,¹⁷ multifunctional,^{2,15} and macroinitiators⁴ have also been employed in the SET-LRP of acrylates. Although structural mimicry provides a starting point for the selection of an appropriate initiator, electronic and reactivity similarities to the dormant polymeric species must also be judiciously considered.

Correspondence to: V. Percec (E-mail: Percec@sas.upenn.edu)

Journal of Polymer Science Part A: Polymer Chemistry, Vol. 49, 1235–1247 (2011) © 2011 Wiley Periodicals, Inc.



SCHEME 1 The initiator and dormant polymeric species in the SET-LRP of MA catalyzed by Cu(0) wire/Me₆-TREN and initiated by (a) MBP and (b) EBiB in DMSO at 25 °C.

In the SET-LRP of methyl acrylate (MA) catalyzed by Cu(0)/hexamethylated tris(2-aminoethyl)amine (Me₆-TREN), both in the case of Cu(0) powder and nonactivated wire, an initial deviation in the molecular weight of the polymer at conversions below 20%^{24–27} was observed, indicating a M_n of poly(methyl acrylate) (PMA) that is higher than the one predicted by a living process. This behavior suggests a pre-equilibrium stage, wherein there is either a lower initial rate of initiation than propagation or a low concentration of Cu(II)X₂ deactivator generated *in situ*.²⁴ This indicates MBP is less reactive than the corresponding dimeric, oligomeric, and polymeric species derived from MA in the SET activation, despite the fact that it is the authentic structural mimic of the monomeric dormant species from MA.

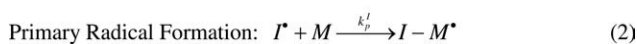
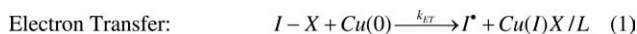
In an effort to design a more effective initiation system for acrylates, it is crucial to correlate and evaluate the structures of some of the most common initiators known for MA with their electronic property and reactivity under SET activation. Here, through computational analysis via energy profile modeling of structures involved in the activation step of SET-LRP, in conjunction with a comparative study between the Cu(0) wire/Me₆-TREN catalyzed SET-LRP of MA initiated with MBP and with ethyl 2-bromoisobutyrate (EBiB), it is demonstrated that EBiB is a more efficient initiator, allowing for an improved dependence of the molecular weight evolution and distribution. Computational and experimental analysis of dibromo derivatives of MBP, dimethyl 2,5-dibromohexandionate (MBHD), and 1,2-bis(bromopropionyloxy)ethane (BPE), and of EBiB, 1,2-bis(bromoisobutyryloxy)ethane (BBiBE), show that these bifunctional initiators offers equally exceptional control over the molecular weight evolution and distribution in the SET-LRP of MA.

RESULTS AND DISCUSSION

The initial deviation in the molecular weight of the polymer at low conversions is an observable deficiency in the SET-

LRP of acrylates initiated with α -halopropionates in polar solvents.^{6,24–27} This suggests a slow initial rate of initiation when compared with propagation or a low concentration of *in situ* generated Cu(II)X₂. A similar observation was reported previously by Sawamoto and coworkers.²⁸ In the ruthenium-mediated LRP of methyl methacrylate (MMA), the observed deviation from theoretical molecular weight at low conversion was attributed to the slower initiation from the monomeric bromide (methyl 2-bromoisobutyrate, MBiB). However, the dimeric model of dormant chain end (MMA-MMA-Br) initiates a faster polymerization than the monomeric counterpart, providing poly(methyl methacrylate) (PMMA) with lower polydispersities and with no deviation from theoretical molecular weight.²⁸ The slow initiation of MBiB can be related to the back strain effect, that is, the release of steric strain of dormant species from rehybridization from sp³ to sp² leading to a higher equilibrium constant.²⁹

In the context of the SET-LRP of MA, slow initiation from MBP can be attributed to either the slow rate of radical formation or lower reactivity of MBP when compared with the oligomeric/polymeric dormant species (MBP-MA, PMA-Br) in the heterogeneous bond dissociation process (Scheme 1). In search for more efficient initiators, computational analysis^{22,30} performed on structures relevant to the dissociative electron transfer (DET) step of SET-LRP was reevaluated, revealing two important trends. First, in comparison with 2-halopropionates, 2-haloisobutyrate demonstrated a lower heterolytic bond dissociation energy (BDE_{hetero}), a decrease in ion-radical pair formation energy (E_{RA}), and an increase in stability of the ion-radical pair (E_{stab}). These should lead to acceleration in the electron transfer step as explained through the sticky dissociative model.^{22,31} The rate enhancement suggests 2-bromoisobutyrate, such as EBiB and MBiB more reactive toward DET, thereby increasing the rate of the electron transfer step (Scheme 2, eq 1). Second, it appears from previous computational studies that the dimeric



SCHEME 2 The initiation process in SET-LRP.^{1,20}

dormant species are more reactive when compared with the corresponding single unit initiator in the activation step under SET-LRP.^{22,30} These preliminary results suggest a closer match in reactivity between EBiB and the dormant polymeric species (EBiB-MA, PMA-Br) derived from MA in the activation step of the SET-LRP (Scheme 1). Thus, previous computational studies^{22,30} inspired us to investigate the relative rates of radical formation from 2-bromopropionate and 2-bromoisobutyrate in the SET-LRP of MA, and so the potential use of 2-bromoisobutyrate as an initiator in SET-LRP of acrylates.

Comparative Analysis of BDE in Pairs of Single Unit Initiators and the Corresponding Dimeric Models

In SET-LRP, activation of the dormant chains occurs through the heterolytic bond cleavage of the carbon-halide bond via a heterogeneous Cu(0)-catalyzed outer-sphere SET process.¹ Herein, the heterolytic BDEs and electron affinities of MBP, MBiB, EBiB, and their corresponding dimeric models with MA under outer-sphere (SET) conditions were investigated using energy profile modeling²² (Fig. 1). The energy of electrostatic E_{RA} is calculated as the difference between the neutral species and ion-radical pair at equilibrium bond length, and the stability of ion-radical pair (E_{stab}) as the difference between the ion-radical pair and the completely separated organic radical and halide leaving group. The lower is the E_{RA} and the stronger is the interaction of the radical with the partial positive charge and the counter-anion halide, the faster is the electron-transfer process. Although MBP and EBiB were examined for direct correlation between computational and experimental analysis of the relative rate of radical formation, MBiB, monomeric mimic of MMA, was selected for consistency with previous work.^{22,30} The comparison of

the $\text{BDE}_{\text{hetero}}$ and electron affinities between the monomeric initiators and the dimeric models would give insight into the relative rates of initiation and propagation.

The calculated bond dissociation energies for the single unit initiators and dimeric mimics are presented in Figure 2 and Table 1. First, in comparison with MBP, the results for MBiB demonstrate a $4.44 \text{ kcal mol}^{-1}$ lower E_{RA} and higher $1.57 \text{ kcal mol}^{-1}$ E_{stab} , in agreement with our previous study.²² Similarly, in EBiB, the E_{RA} is higher by $4.23 \text{ kcal mol}^{-1}$ and the E_{stab} by $1.48 \text{ kcal mol}^{-1}$ than in MBP. Increased stabilization of the ion-radical pair results in a significant acceleration in the electron-transfer process via the sticky dissociative model. This means that 2-haloisobutyrate such as EBiB and MBiB are more reactive during the activation step of SET-LRP when compared with 2-halopropionates such as MBP.

Second, when comparing between MBP and the corresponding dimeric species (syn and anti), there is a $2.52\text{--}3.05 \text{ kcal mol}^{-1}$ decrease in E_{RA} and $0.83\text{--}1.69 \text{ kcal mol}^{-1}$ increase in E_{stab} in the dimeric mimics. This indicates the MBP-MA dimers are better electron acceptor, thus more reactive toward DET than the single unit MBP. Although the trend is conserved for MBiB and EBiB, the E_{RAS} of the radical anion and of the dimeric model are more similar. Specifically, the decrease in E_{RA} is 1.68 and $0.11 \text{ kcal mol}^{-1}$ in MBiB and EBiB, respectively, when compared with their corresponding dimers. Similarly, the E_{stab} does not increase significantly in the dimeric models of MBiB and EBiB, demonstrated by a difference of 0.43 and $1.43 \text{ kcal mol}^{-1}$, respectively. Third, our preliminary computational study of the trimer species unveils marginal increase in the relative reactivity between dimeric and trimeric species derived from MBP and EBiB. For example, the results for EBiB-MA-MA show a 0.4-kcal mol^{-1} lower E_{RA} and 1 kcal mol^{-1} higher E_{stab} when compared with those of EBiB-MA (Table 1). Consistent with our expectations, these results suggest that the reactivity of 2-haloisobutyrate matches better with the reactivity of dormant species of MA on the DET step of SET-LRP of MA, with the later being only slightly more reactive. In other words,

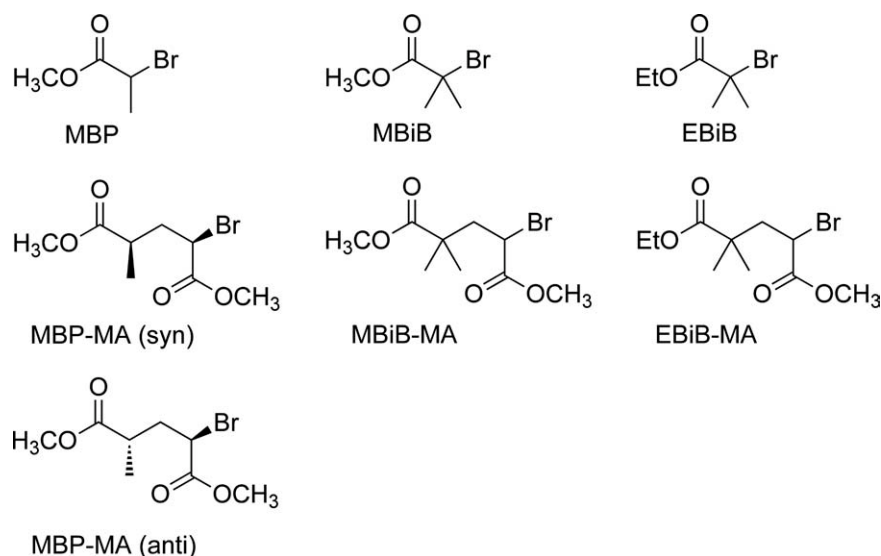


FIGURE 1 Single unit monofunctional initiators and the corresponding dimers.

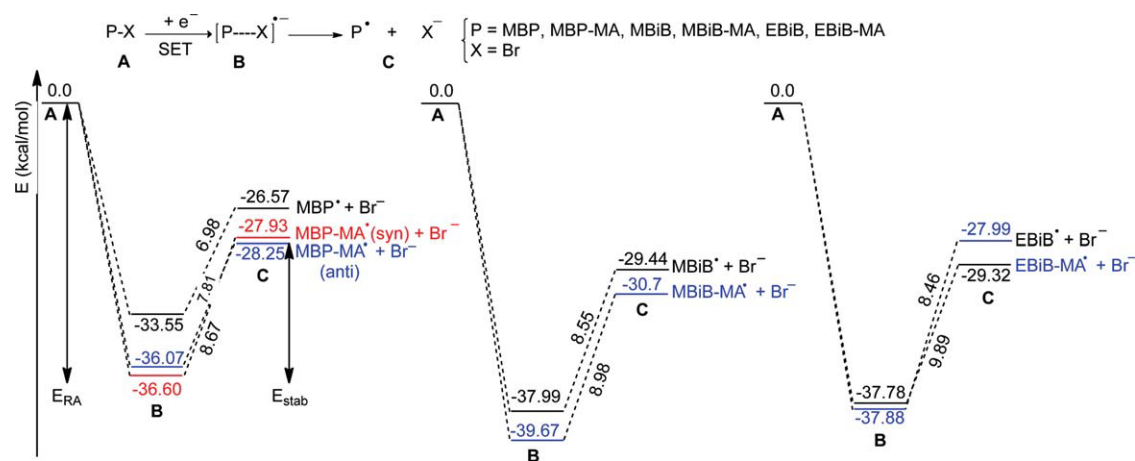


FIGURE 2 E_{RA} and the E_{stab} for the single unit monofunctional initiators and dimeric models.

despite the structural difference, on the basis of electronics and reactivity, EBiB and MBiB are the true electronic chain-end mimics of the dimeric and oligomeric dormant species of MA.

Comparative Analysis of BDE of a Bifunctional Initiator and Its Dimeric Derivatives

The results presented above suggest that the dimeric species such as MBP-MA or EBiB-MA are better models to predict the BDE of the polymer dormant species P-X under SET-LRP conditions when compared with the monomer counterparts.

This inspired us to investigate the formation of radicals from MBHD, a bifunctional initiator that structurally resembles the dimer MA-MA-Br species, [Fig. 3(b)] relative to its dimeric species with MA [Fig. 3(a)] under SET activation. Because of the presence of multiple stereocenters, all diastereomers of the bifunctional initiator and its dimers with MA were subjected to computational analysis to account for the effect of stereochemistry.

The relative energies of heterolytic bond dissociation energies and of the formation and decomposition of radical anion

TABLE 1 Dormant Chain-End Bond Dissociation Energies Modeled at the B3LYP/6-31+G* level

Entries	Compounds	E_{homo} (kcal mol ⁻¹)	E_{hetero} (kcal mol ⁻¹)	E_{RA} (kcal mol ⁻¹)	E_{stab} (kcal mol ⁻¹)
1	MBP	55.99	-26.57	-33.55	6.98
2	MBiB	53.11	-29.44	-37.99	8.55
3	EBiB	53.23	-29.32	-37.78	8.46
4	MBP-MA (anti)	54.30	-28.25	-36.07	7.81
5	MBP-MA (syn)	54.62	-27.93	-36.60	8.67
6	MBP-MA-MA	54.15	-28.41	-38.22	9.81
7	MBiB-MA	51.86	-30.70	-39.67	8.98
8	EBiB-MA	54.56	-27.99	-37.88	9.89
9	EBiB-MA-MA	55.17	-27.38	-38.27	10.88
10	MBHD-1 (S-R)	53.33	-29.23	-42.95	13.72
11	MBHD-2 (S-S)	54.14	-28.41	-43.37	14.95
12	MBHD1-MA-1 (S-S-R)	51.93	-30.62	-51.92	21.29
13	MBHD1-MA-1 (S-S-R)	52.18	-30.38	-38.83	8.45
14	MBHD1-MA-2 (S-S-S)	53.00	-29.55	-45.90	16.35
15	MBHD1-MA-2 (S-S-S)	53.56	-28.99	-38.57	9.58
16	MBHD2-MA-1 (S-R-R)	53.14	-29.41	-44.77	15.36
17	MBHD2-MA-1 (S-R-R)	52.81	-29.74	-40.77	11.03
18	MBHD2-MA-2 (S-R-S)	56.18	-26.38	-43.96	17.58
19	MBHD2-MA-2 (S-R-S)	55.40	-27.16	-37.04	9.88
20	MBHD2-MA-1 (S-R-R)	53.14	-29.41	-44.77	15.36
21	MBHD-MA ^a	53.52	-29.03	-42.72	13.69

^a E_{average} of all diastereomers.

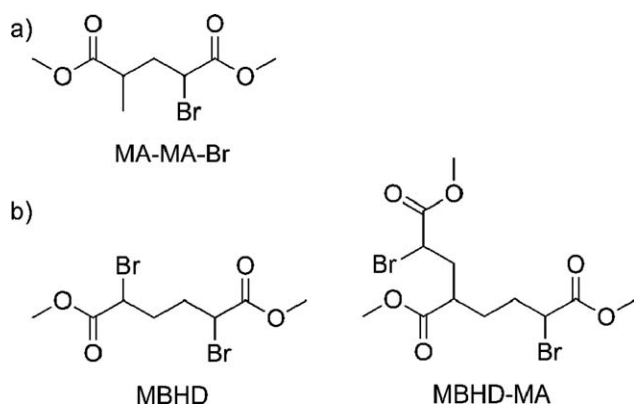


FIGURE 3 (a) Dimeric model of the dormant chain. (b) Single unit bifunctional initiator and the corresponding dimers.

intermediates for MBHD and MBHD-MA are presented in Table 1, entries 10–20 and in Figure 4. The results for the electron affinities of the MBHD-MA dimers are averaged because the initiator itself is not diastereomerically enriched. First, the reactivity of MBHD is significantly higher than that of the monofunctional initiators, MBP and EBiB under SET activation, as shown by a much lower E_{RA} and greater E_{stab} (Fig. 4). Second, the trend is clear that the reactivity of the bifunctional initiator MBHD is very close to that of its dimers with MA. This is illustrated by the essentially identical E_{hetero} and small differences in E_{RA} and E_{stab} between the dimeric and trimeric species derived from MBHD (Fig. 4).

In short, computational studies demonstrate that 2-haloisobutyrate, such as EBiB, are more reactive than MBP in the activation process of SET-LRP because of a lower BDE and better stabilization of the ion-radical pair leading to an accelerated electron transfer process. In addition, EBiB exhibits similar reactivity with the corresponding dormant polymeric species. Therefore, 2-haloisobutyrate should serve as more efficient initiators than MBP in the SET-LRP of MA. Further, the results suggest that a bifunctional initiator such as MBHD could be effective in the SET-LRP of acrylates because of its enhanced reactivity that matches well with that of the dormant polymeric species. Hence, the Cu(0) wire/Me₆-TREN catalyzed SET-LRP of MA initiated with EBiB and MBHD were evaluated in comparison with the SET-LRP of MA initiated with MBP.

Comparison of Apparent Rate Constants of Propagation (k_p^{app}) in the SET-LRP of MA Initiated with MBP and EBiB

Figure 5(a) shows the overlapped kinetic plots for the Cu(0) wire/Me₆-TREN catalyzed SET-LRP of MA initiated with MBP in dimethyl sulfoxide (DMSO) at 25 °C under the following conditions: [MA]/[MBP]/[Me₆-TREN] = 222/1/0.1. Figure 5(c) depicts the kinetic plots for the SET-LRP of MA initiated with EBiB under identical conditions. Both polymerizations clearly exhibited first order kinetics, indicative of a living polymerization. The SET-LRP of MA initiated with EBiB, with an apparent rate constant $k_p^{app} = 0.069 \text{ min}^{-1}$, proceeded only slightly slower than that initiated with MBP ($k_p^{app} =$

0.073 min^{-1} ; Table 2, entries 1 and 2). Thus, the choice of a 2-bromopropionate or 2-bromoisobutyrate as the initiator does not affect significantly the kinetics of the polymerization.

M_w/M_n versus Conversion in the SET-LRP of MA Initiated with MBP and EBiB

The evolution of the number average molecular weight (M_n) and of the molecular weight distribution (M_w/M_n) versus theoretical molar mass calculated for a LRP process (M_{th}) of PMA for the Cu(0) wire/Me₆-TREN catalyzed SET-LRP of MA initiated with MBP and with EBiB are depicted in Figure 5(b,d). For the SET-LRP of MA initiated with MBP, an initial deviation in the molecular weight of polymer is detected at conversions below 15%. This is consistent with what was observed previously for kinetic experiments performed with Cu(0) powder. When using EBiB as the initiator, there is no deviation in the polymer molar mass from theoretical values at all conversions. This enhanced control over the molecular weight distribution effectively overcomes the major challenge in the SET-LRP of acrylates initiated with 2-haloisobutyrate. As the deviation from theoretical molecular weights could be attributed to a lower rate of initiation than propagation,²⁴ it suggests a faster rate of activation in the SET-LRP of MA initiated by EBiB than by MBP. This is consistent with recent findings that the use of highly activated Cu(0) wire increases the SET activation, leading to a complete elimination of the

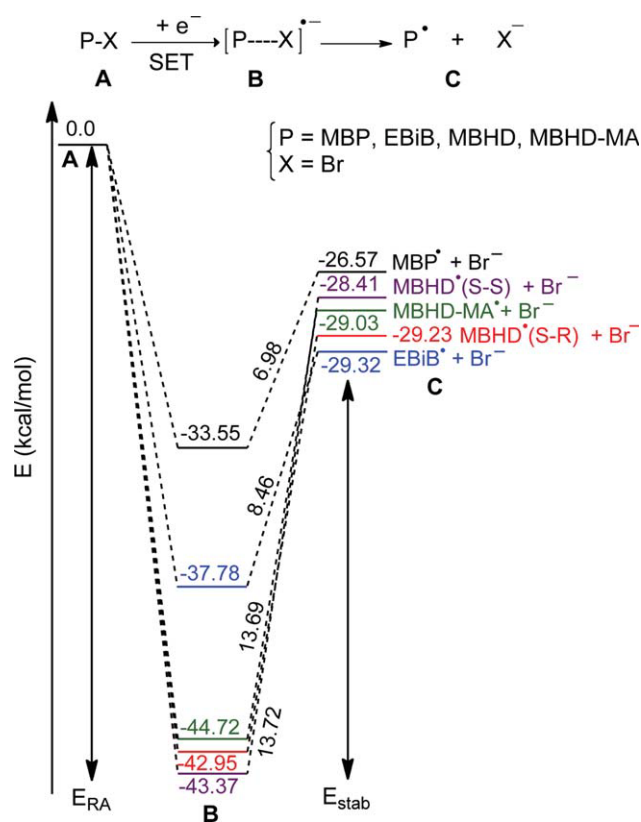


FIGURE 4 E_{RA} and the E_{stab} for the single unit initiators and dimeric models.

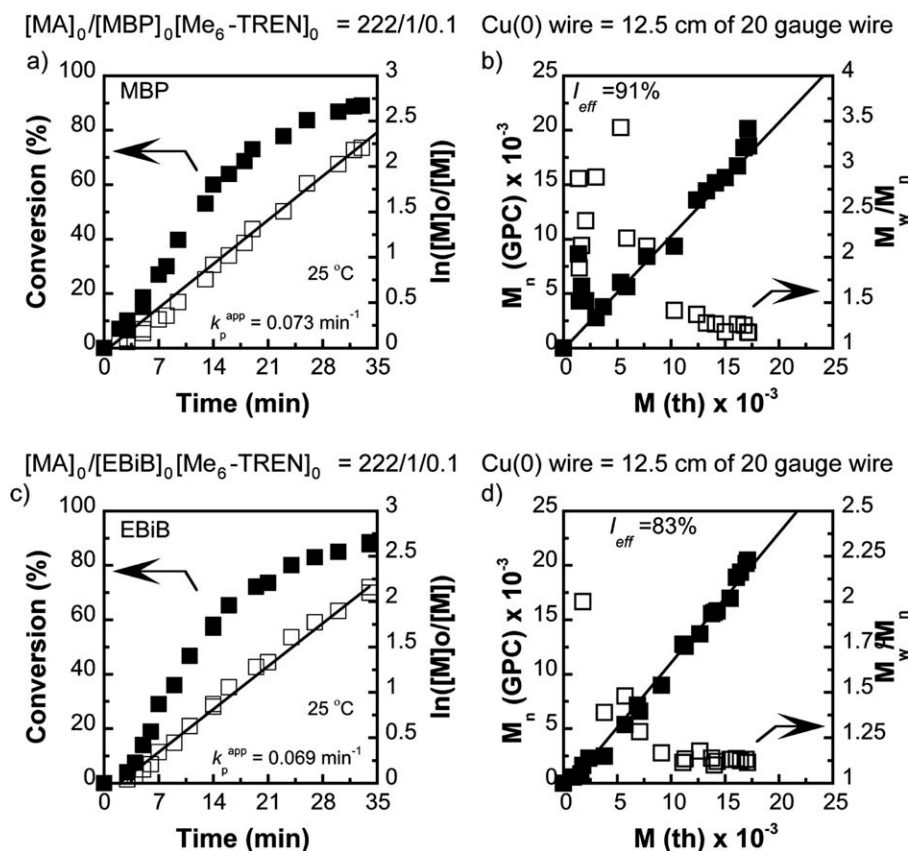


FIGURE 5 Kinetic plots and molecular weight evolutions for SET-LRP of MA initiated with (a and b) MBP and (c and d) EBiB in DMSO at 25 °C. Reaction conditions: MA = 1 mL, DMSO = 0.5 mL, $[MA]/[Initiator]/[Me_6-TREN] = 222/1/0.1$. Cu(0) wire = 12.5 cm of 20 gauge wire.

observed deviation from theoretical molar masses at low conversions.³²

The enhanced control over molecular weight distribution when using EBiB as the initiator is further demonstrated by the fact that narrower molecular weight distribution is achieved when EBiB is employed as the initiator, indicated by the M_w/M_n values of <1.2 at monomer conversions of above 50% and of 1.11 at ~89% conversion (as compared to that of 1.17 obtained at the same monomer conversion in the SET-LRP of MA initiated with MBP; Table 2, entries 1 and 2).

Initiator Consumption

In atom transfer radical polymerization (ATRP), 2-bromoisobutyrate have been shown to generate initiating radicals faster than the corresponding 2-halopropionates because of the better stabilization of the generated tertiary radicals.²³ The ATRP equilibrium constant, K_{ATRP} , of EBiB is ~30 times higher than for MBP.³³ In addition, the current computational analysis on the heterolytic BDEs involved in the activation process of SET-LRP confirmed the higher reactivity of EBiB as compared to MBP toward DET. To investigate the relative rates of consumption of MBP and EBiB under SET-LRP conditions the initiator consumption experiments were conducted

TABLE 2 SET-LRP of MA Catalyzed by Cu(0)/ Me_6 -TREN in DMSO at 25 °C

Entries	Initiators	Time (min)	Conversion (%)	k_p^{app} (min^{-1})	M_n (GPC)	M_w/M_n	I_{eff} (%)
1 ^a	MBP	33	89	0.073	18,545	1.17	91
2 ^a	EBiB	34	88.5	0.069	20,171	1.11	83
3 ^{b,c}	MBHD	42	90	0.061	38,882	1.09	96
4 ^{b,c}	BPE	40	89	0.060	36,061	1.11	90
5 ^{b,c}	BBiBE	38	85	0.061	35,820	1.09	97
6 ^{b,d}	MBHD ³²	15	82	0.126	30,625	1.11	96
7 ^{b,d}	BPE ³²	16	86	0.132	30,890	1.11	95
8 ^{b,d}	BBiBE	21	88	0.107	36,047	1.10	93

^a $[MA]/[Initiator]/[Me_6-TREN] = 222/1/0.1$.

^b $[MA]/[Initiator]/[Me_6-TREN] = 444/1/0.2$.

^c Commercial Cu(0) wire.

^d Activated Cu(0) wire.

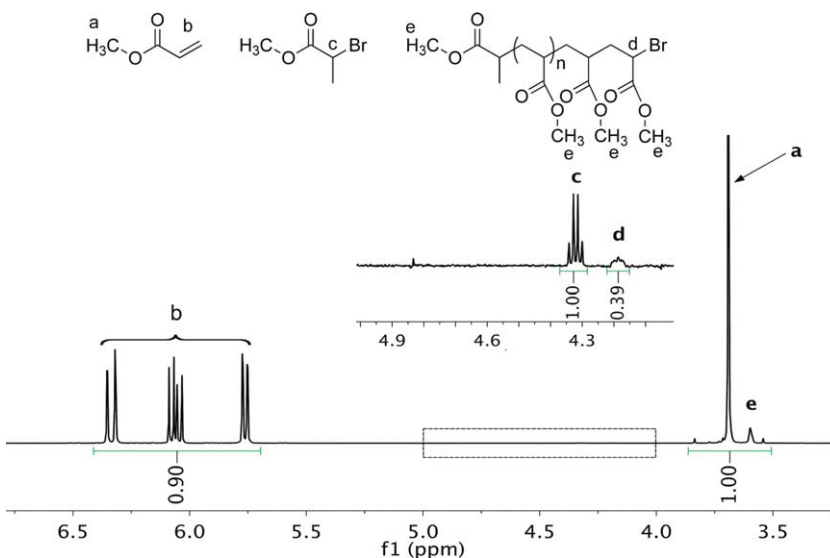


FIGURE 6 500-MHz ^1H NMR spectrum of PMA at 10% conversion. Polymerization conditions: MA = 1 mL, DMSO = 0.5 mL, [MA]/[MBP]/[Me₆-TREN] = 222/1/0.1. Cu(0) wire = 12.5 cm of 20 gauge wire.

using ^1H NMR spectroscopy. The polymerization conditions were as followed: MA = 1 mL, DMSO = 0.5 mL, [MA]/[Initiator]/[Me₆-TREN] = 222/1/0.1/1; Cu(0) wire = 12.5 cm of 20 gauge wire.

Figure 6 shows a 500-MHz ^1H NMR spectrum of one of the PMA samples isolated in the SET-LRP of MA initiated with MBP. The comparison of the integrals of the signals of the monomer vinyl signals (5.7–6.4 ppm) over the polymeric $-\text{OCH}_3$ signal (3.65 ppm) indicates 10% monomer conversion after 3 min. The inset of Figure 6 shows a sharp quartet at approximately 4.3–4.35 ppm representative of the proton located at the α position of the bromide atom of the MBP initiator (H_c) and a broad signal at 4.2 ppm corresponding to the proton $-\text{CH}-$ located at the α position of the bromide chain end of PMA (H_d). This means that at 10% monomer conversion $\sim 28\%$ of the initial initiator was consumed. The same analysis for different samples indicates that the initia-

tion step was complete at $\sim 34\%$ monomer conversion. This is comparable with the rate of initiator consumption observed previously in the SET-LRP of MA initiated by MBP and catalyzed by Cu(0) powder.²⁴

The evaluation of initiator consumption in the SET-LRP of MA initiated with EBiB was conducted under identical conditions. DMF was added as internal standard at 1/1 molar ratio to the initiator (EBiB) because of the overlapping in chemical shift between the initiator and the polymeric protons. Figure 7 shows a 500-MHz ^1H NMR spectrum of PMA sample isolated at 4% conversion. A sharp quartet at ~ 4.15 ppm represents the initiator $-\text{OCH}_2\text{CH}_3$ (H_c) protons which overlaps with the polymer $-\text{CH}-$ (H_f) proton located at the α position of the bromide chain end of PMA. A broad signal at 4 ppm corresponds to the polymer $-\text{OCH}_2\text{CH}_3$ (H_d) proton. The inset from the 7.5–8.25 ppm region shows a sharp singlet at 7.92 ppm corresponding to H_g of DMF. The

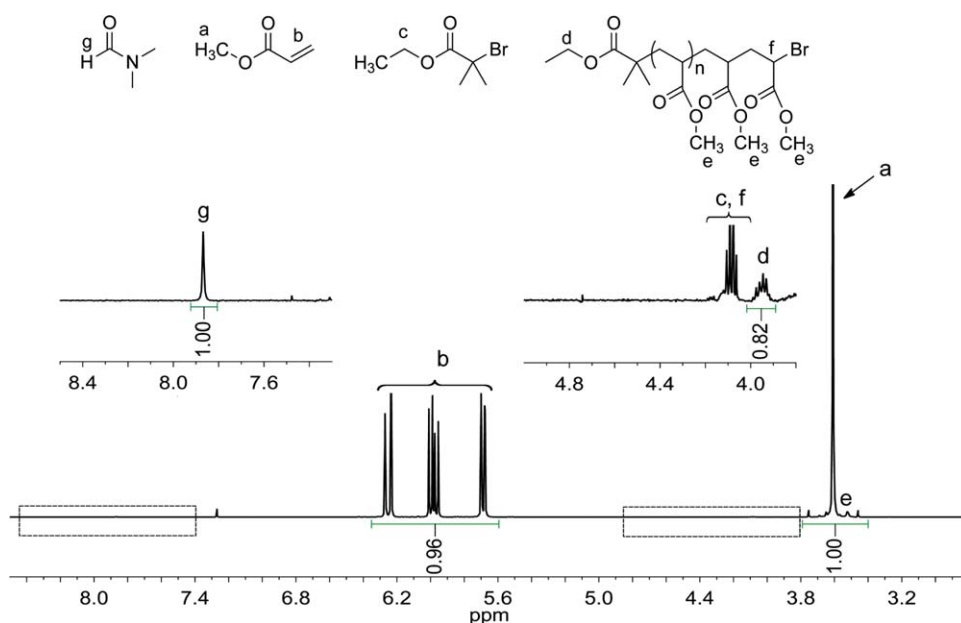


FIGURE 7 500-MHz ^1H NMR spectrum of PMA at 4% conversion. Polymerization conditions: MA = 1 mL, DMSO = 0.5 mL, [MA]/[EBiB]/[Me₆-TREN]/[DMF] = 222/1/0.1/1. Cu(0) wire = 12.5 cm of 20 gauge wire.

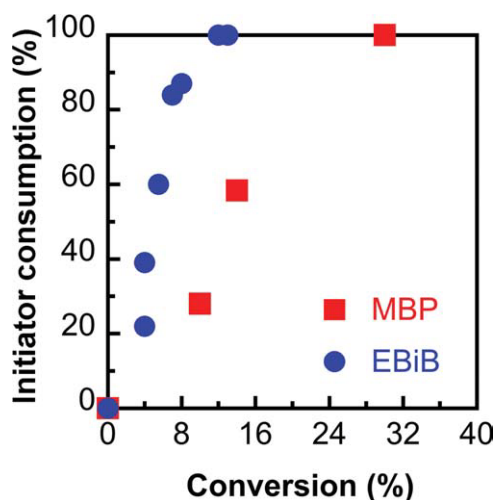


FIGURE 8 Initiator consumptions in SET-LRP of MA initiated with MBP and EBiB in DMSO at 25 °C. Reaction conditions: MA = 1 mL, DMSO = 0.5 mL, [MA]/[Initiator]/[Me₆-TREN] = 222/1/0.1. Cu(0) wire = 12.5 cm of 20 gauge wire.

consumption of initiator is calculated as: $\frac{H_f}{2H_g} \times 100\%$. Here, ~41% of the initiator was consumed at 4% monomer conversion. The same analysis on reaction samples at later time points in the polymerization indicated that the initiation step is complete at ~12% monomer conversion (Fig. 8).

Figure 8 compares the rates of initiator consumption in the SET-LRP of MA conducted in DMSO. Consistent to the results from computational analysis, it is clear that EBiB is consumed much faster than MBP under the current SET-LRP conditions because of its enhanced reactivity in the DET step (Scheme 2, eq 1).

Initiator Efficiency

Despite the enhanced control over the molecular weight distribution, the initiator efficiency of EBiB ($I_{\text{eff}} = 83\%$) is noticeably lower than that of MBP ($I_{\text{eff}} = 91\%$) [Fig. 5(b,d)]. This might be attributed to the competing effects between DET and primary radical formation (Scheme 2). It must be noted that although EBiB is more active than MBP in the heterogeneous dissociation (Scheme 2, eq 1), the resulting 3° radical is thermodynamically more stable than the 2° radical formed from the latter. As a result, it is likely that the rate constant of addition of the EBiB[•] radical to MA is slower than that of the MBP[•] radical to MA, demonstrated by a decrease in the enthalpy of primary radical formation from EBiB when compared with MBP (Scheme 3, eqs 3 and 4). In theory, this would lead to an increase in the likelihood for side reactions such as dimerization, thus, decreasing the initiator efficiency. As there are no direct experiments to test



SCHEME 3 Primary radical formation in SET-LRP.

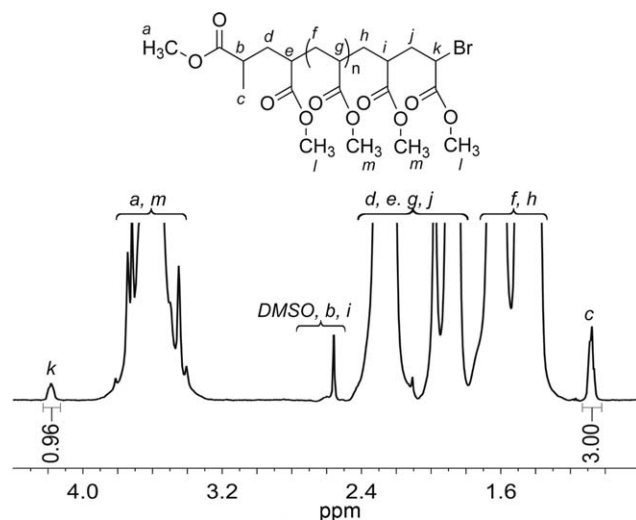


FIGURE 9 ¹H NMR spectrum at 500 MHz of PMA at 89% conversion ($M_n = 18545$ and $M_w/M_n = 1.17$). Polymerization conditions: MA = 1 mL, DMSO = 0.5 mL, [MA]/[MBP]/[Me₆-TREN] = 222/1/0.1. Cu(0) wire = 12.5 cm of 20 gauge wire.

this hypothesis, kinetic modeling studies may be required to deconvolute these two processes.

Chain-End Analysis

Complete retention of chain-end functionality is necessary to achieve ultrahigh molar mass polymers and allows for the preparation of macroinitiators for block copolymerizations. For 2-haloisobutyrate to be a suitable replacement of 2-halopropionates, it is necessary to monitor and compare the retention of chain end functionality of the PMA samples prepared from the SET-LRP of MA initiated by MBP and EBiB.

Figure 9 shows the 500-MHz ¹H NMR spectrum of the isolated PMA sample ($M_n = 18,545$ and $M_w/M_n = 1.17$) obtained at 89% monomer conversion from the Cu(0) wire/

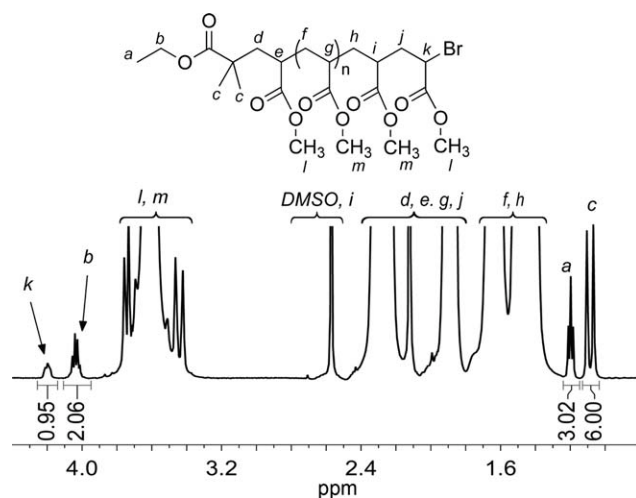


FIGURE 10 ¹H NMR spectrum at 500 MHz of PMA at 88% conversion ($M_n = 20480$ and $M_w/M_n = 1.11$). Polymerization conditions: MA = 1 mL, DMSO = 0.5 mL, [MA]/[EBiB]/[Me₆-TREN] = 222/1/0.1. Cu(0) wire = 12.5 cm of 20 gauge wire.

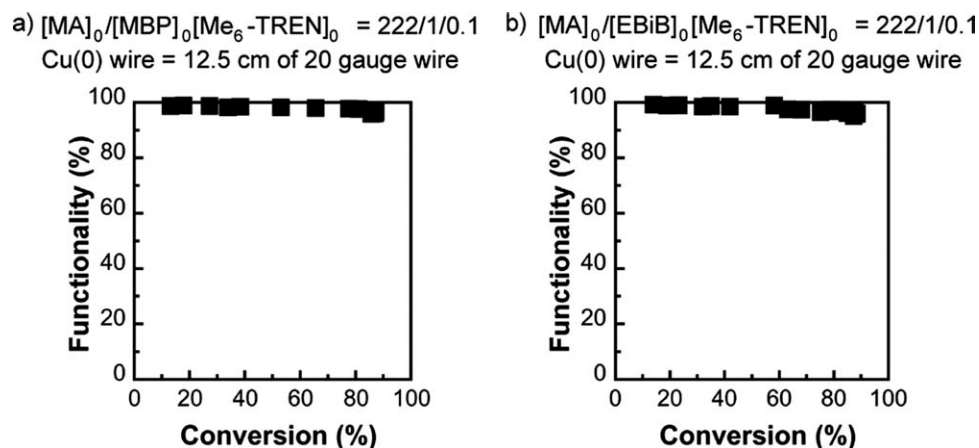


FIGURE 11 The percentage of bromine-functionalized chains versus conversion (%) for the SET-LRP of MA initiated with (a) MBP and (b) EBiB in DMSO at 25 °C. Reaction conditions: MA = 1 mL, DMSO = 0.5 mL, $[MA]/[Initiator]/[Me_6-TREN] = 222/1/0.1$. Cu(0) wire = 12.5 cm of 20 gauge wire.

Me_6 -TREN catalyzed SET-LRP of MA initiated with MBP in DMSO at 25 °C. The percentage of chain-end functionality can be estimated by a comparison of the integrals of the peaks H_c (corresponding to the initiator CH_3 groups) and H_k (proton CH located in the α -position of the bromine chain end; eq 5).

$$f(\%) = \left[\frac{H_k}{H_c/3} \right] \times 100 \quad (5)$$

Consistent with previous results,^{17,24,26} the Cu(0) wire/ Me_6 -TREN catalyzed SET-LRP of MA initiated with MBP exhibits very high retention of chain end functionality, indicated by high functionality [f (%)] values, $f > 96\%$, throughout the polymerization [Fig. 11(a)].

Similar analysis was applied for the PMA samples from the SET-LRP of MA initiated with EBiB conducted under identical conditions. Figure 10 shows the 500-MHz 1H NMR spectrum of the PMA sample isolated at 88% monomer conversion. The percentage of chain-end functionality can be estimated by a comparison of the integrals of the peaks H_c (corresponding to the initiator CH_3 groups) and H_k (proton CH located in the α -position of the bromine chain end; eq 6).

$$f(\%) = \left[\frac{H_k}{H_c/6} \right] \times 100 \quad (6)$$

Figure 11(b) shows that in this depicted representative polymerization, f is high through out the polymerization, culminating in PMA sample with $f > 94\%$. Considering the experimental error of our NMR method, this value confirms a polymer with high retention of functional chain ends.³⁴

Both SET-LRP of MA initiated with MBP and EBiB allows for high retention of functional chain ends. This suggests that both can be used in the synthesis of functionally terminated polymers. Further optimization of SET-LRP to ensure extremely high functionality may require addition of the external deactivator ($Cu(II)X_2$)^{16,24} or tailoring of the polymerization rates via activation of Cu(0) wire,³² manipulation of Cu(0) surface area²⁶ or ligand concentration.³⁵ This will be addressed in our upcoming publication.

Structural Analysis of PMA by MALDI-TOF

MALDI-TOF analysis confirmed that the SET-LRP of MA initiated with MBP or α -halopropionate derivatives produces polymers with perfect chain end functionality.^{1,2,15,17,24} Here, matrix-assisted laser desorption/ionization — time-of-flight mass spectrometry (MALDI-TOF-MS) was applied to examine low molecular weight PMA isolated at 71% in the SET-LRP using EBiB as the initiator.

The MALDI-TOF spectrum (Fig. 12) exhibits only one series of peaks of which interval was periodic at 86.2, the molar mass of the MA monomer. The lack of a secondary mass

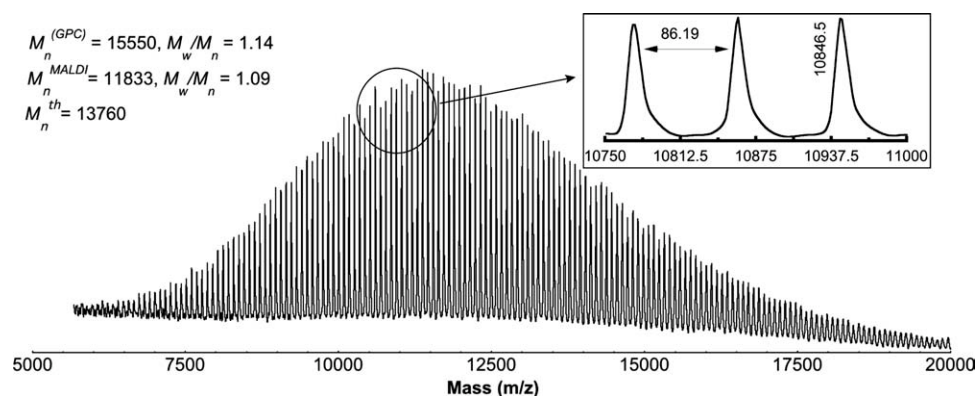


FIGURE 12 MALDI-TOF-MS spectrum of PMA obtained at 71% conversion by the polymerization of MA initiated with EBiB in DMSO at 25 °C. Reaction conditions: MA = 1 mL, DMSO = 0.5 mL, $[MA]/[EBiB]/[Me_6-TREN] = 222/1/0.1$. Cu(0) wire = 12.5 cm of 20 gauge.

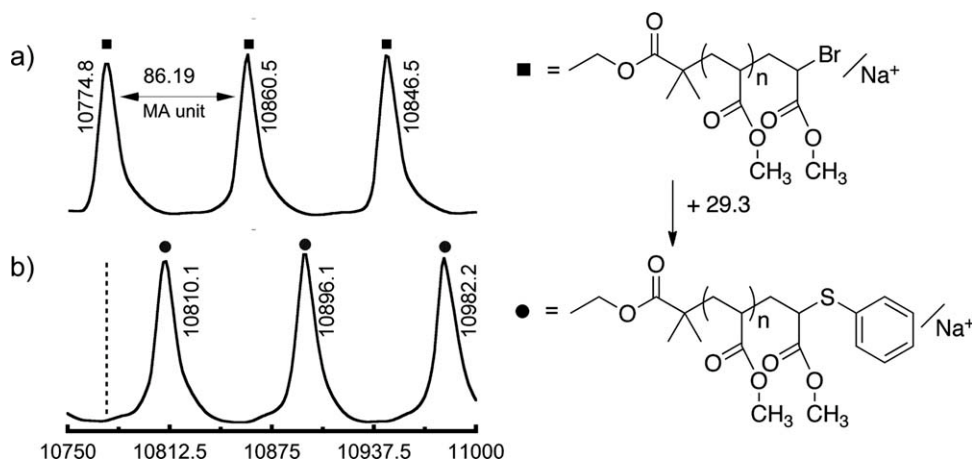


FIGURE 13 MALDI-TOF-MS spectra of (a) PMA obtained at 71% conversion by the polymerization of MA initiated with EBiB in DMSO at 25 °C. $[MA]/[EBiB]/[Me_6-TREN] = 222/1/0.1$; (b) PMA end capped with thiophenol.

peak series in the spectrum indicates the absence of irreversible termination. From Figure 13, M_{th} of PMA obtained at 71% conversion was 13,760, and MALDI-TOF analysis provided M_n of 11,833 ($M_w/M_n = 1.09$). This result demonstrates a relatively good agreement between the theoretical and experimental values of M_n . Retention of chain end functionality was confirmed by functionalization of PMA by thioesterification with thiophenol. MALDI-TOF analysis was carried out on PMA end capped with thiophenol to confirm the end capping reaction and the absence of halogen loss during polymerization (Fig. 13). It can be seen that the previous distribution corresponding to the halogen terminated PMA was totally absent and the new distribution appears ~ 29.3 mass units above the previous. Thus, the thiophenol functionalization experiment demonstrates the functional structure of the chain end by SET-LRP using EBiB initiator.

SET-LRP of MA Initiated with Bifunctional Initiators

As predicted from our computational analysis, the reactivity of a bifunctional derivative of 2-bromopropionate, such as MBHD, is much higher than that of its monofunctional counterpart, MBP, and closely matches that of the corresponding polymeric dormant species in the activation process of SET-LRP. As bifunctional initiators are particularly valuable in the synthesis of telechelic polymers,^{17,36} or of dendritic macromolecules via TERMINI concept,^{37–40} understanding the kinetic behaviors of the SET-LRP using MBHD as the initiator is of great interest.

As depicted from Figure 14, the SET-LRP of MA initiated with MBHD in DMSO at 25 °C exhibits first order kinetics, demonstrating a living polymerization, and most importantly, exceptional dependence of the molecular weight evolution and distribution with conversions. Unlike the SET-LRP of MA initiated with MBP under identical conditions, there is no deviation in the polymer molecular weight from theoretical values at low conversions. This improved control, over molecular weight distribution, supports our computational results.

Interestingly, the absence of an initial deviation in the polymer molar mass from theory at low conversions was also observed in the SET-LRP of MA initiated with BPE and BBiBE under identical conditions (Figs. 15 and 16). In addition, the polymers prepared from the SET-LRP of MA initiated with all bifunctional initiators in this study exhibit narrow molecular weight distribution at high conversions ($M_w/M_n = \sim 1.11$ at $\sim 89\%$; Table 2, entries 3, 4 and 5). Thus, the combined computational and experimental analyses suggest that MBHD, BPE, and BBiBE are effective initiators for the SET-LRP of acrylates.

Toward perfection of the current SET-LRP methodology as a catalytic platform for the synthesis of tailored polymers, it is of great interest to combine the desirable attributes offered by bifunctional initiators, and the dramatic rate acceleration and improved predictability in the molecular weight evolution by activated Cu(0) wire. Consistent with our previous

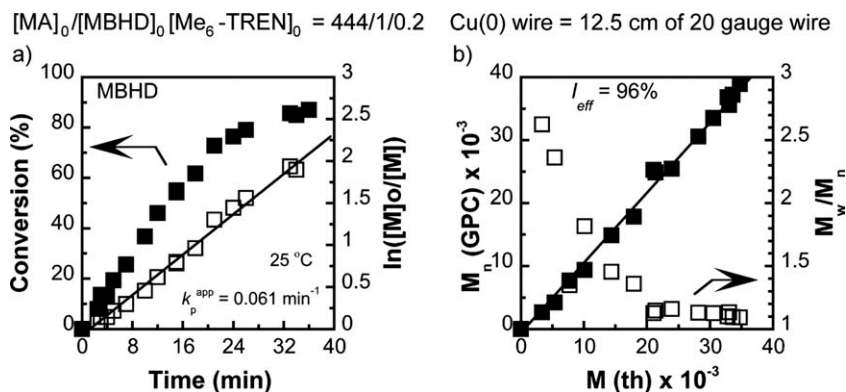


FIGURE 14 Kinetic plots and molecular weight evolutions for SET-LRP of MA initiated with MBHD in DMSO at 25 °C. Reaction conditions: MA = 1 mL, DMSO = 0.5 mL, $[MA]/[MBHD]/[Me_6-TREN] = 444/1/0.2$. Cu(0) wire = 12.5 cm of 20 gauge wire.

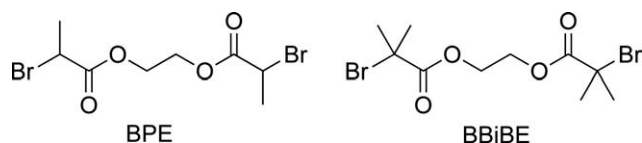


FIGURE 15 Bifunctional initiator derivatives of MBP and EBiB.

publication on the use of MBHD and BPE in SET-LRP in conjunction with activated Cu(0) wire,³² the SET-LRP of MA initiated with BBiBE and catalyzed by activated Cu(0) wire proceeded at a comparable rate ($k_p^{app} = 0.107 \text{ min}^{-1}$) and exhibited exceptional dependence of the molecular weight evolution with conversion and very narrow molecular weight distribution (Fig. 17; Table 2, entry 8).

CONCLUSIONS

The Cu(0) wire/ $\text{Me}_6\text{-TREN}$ catalyzed SET-LRP of MA initiated with a 2-bromoisobutyrate, EBiB, was evaluated in comparison with the SET-LRP of MA using a 2-bromopropionate, MBP, as the initiator. The SET-LRP of MA initiated with EBiB in DMSO proceeds at a comparable rate as that initiated with MBP. It exhibits improved predictability and dependence of molecular weight evolution and distribution as a function of conversions, exemplified by the absence of a deviation in the polymer molecular weight from the theoretical values at all conversions. This improved control can be attributed to the higher reactivity of EBiB and its similar

reactivity to the polymeric dormant species toward DET in the activation process of SET-LRP. ^1H NMR and MALDI-TOF experiments provided structural analysis in support of retention of chain-end functionality in the SET-LRP process using both initiators. The combined computational and experimental analyses also demonstrated that not only EBiB, but also MBHD, BPE, and BBiBE are effective in initiating well-controlled SET-LRP of MA and are expected to be compatible for other functional acrylates. The use of activated Cu(0) wire in the SET-LRP of acrylates initiated bifunctional initiators, which further improve the perfection of the current SET-LRP methodology through dramatic rate acceleration, although still allowing for exceptional predictability and dependence of molecular weight evolution and distribution with conversion.

EXPERIMENTAL

Materials

MA (99%, Acros) was passed over a short column of basic Al_2O_3 before use to remove the radical inhibitor. Copper (0) wire (20 gauge, Fischer), EBiB (98%, Acros), and MBP (99%, Acros) were used as received. DMSO (99.9%, Fisher, certified ACS) was distilled under reduced pressure before use. $\text{Me}_6\text{-TREN}$ was synthesized as described in the literature.⁴¹ The bifunctional initiator BPE was synthesized by esterification of ethylene glycol with 2-bromopropionyl bromide in the presence of pyridine.¹⁷ BBiBE was synthesized as described

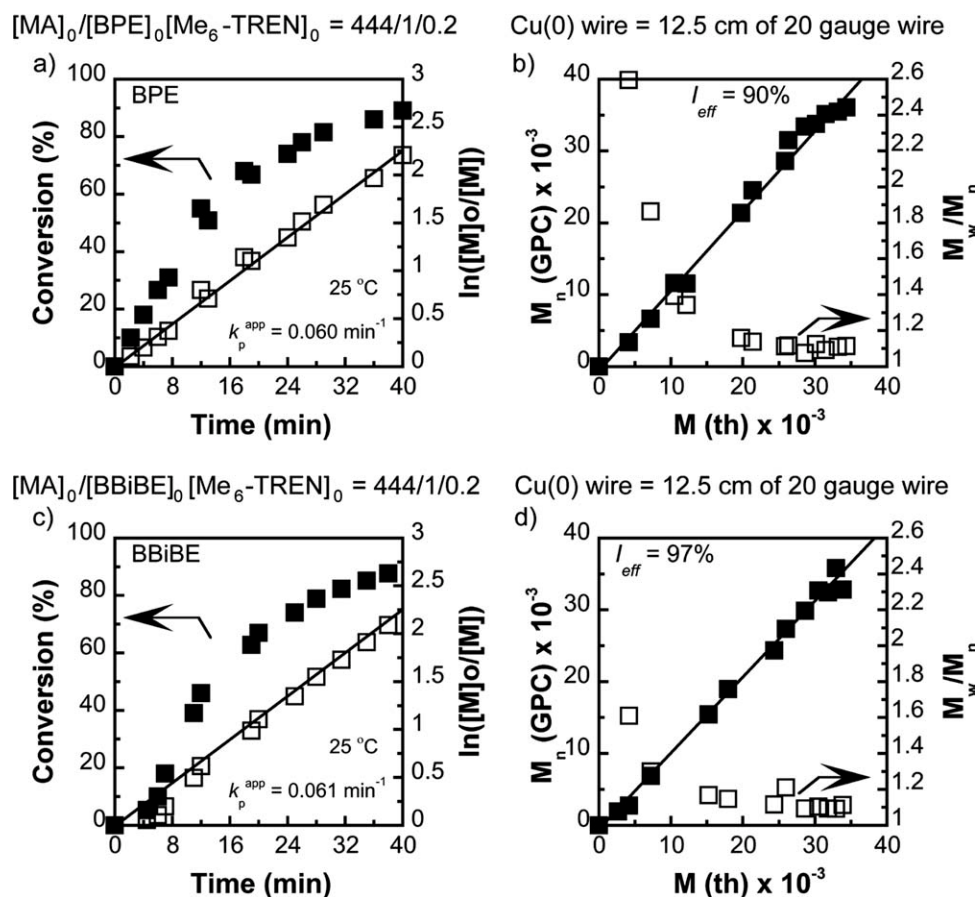


FIGURE 16 Kinetic plots and molecular weight evolutions for SET-LRP of MA initiated with (a and b) BPE and (c and d) BBiBE in DMSO at 25 °C. Reaction conditions: MA = 1 mL, DMSO = 0.5 mL, $[\text{MA}]/[\text{Initiator}]/[\text{Me}_6\text{-TREN}] = 444/1/0.2$. Cu(0) wire = 12.5 cm of 20 gauge wire.

$[MA]_0/[BBiBE]_0/[Me_6-TREN]_0 = 444/1/0.2$ Activated Cu(0) wire = 12.5 cm of 20 gauge wire

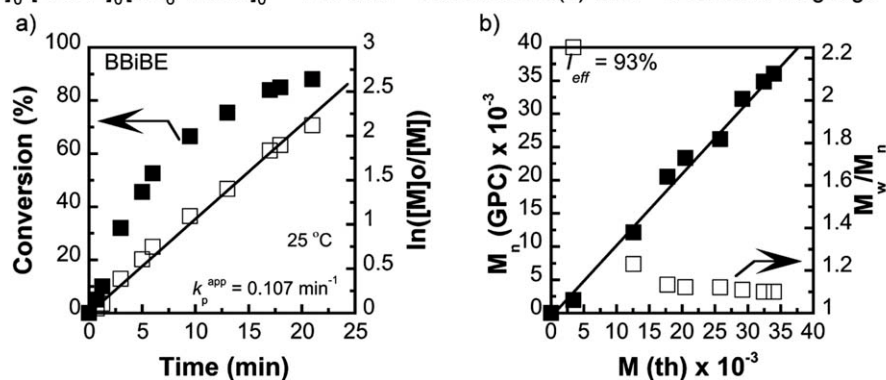


FIGURE 17 Kinetic plots and molecular weight evolutions for SET-LRP of MA initiated with BBiBE in DMSO at 25 °C. Reaction conditions: MA = 1 mL, DMSO = 0.5 mL, $[MA]/[BBiBE]/[Me_6-TREN] = 444/1/0.2$. Activated Cu(0) wire = 12.5 cm of 20 gauge wire.

in the literature.⁴² MBHD was prepared as described in a previous publication.⁴³

Techniques

¹H NMR spectra at 500 MHz were recorded on a Bruker DRX500 NMR instrument at 20 °C in CDCl₃ with tetramethylsilane as internal standard. Gel permeation chromatography (GPC) analysis of the polymer samples were done on a Perkin-Elmer Series 10 high-performance liquid chromatography (HPLC), equipped with an LC-100 column oven (30 °C), a Nelson Analytical 900 Series integration data station, a Perkin-Elmer 785 UV-vis detector (254 nm), a Varian star 4090 refractive index detector, and three AM gel columns (500 Å, 5 μm; 1000 Å, 5 μm; and 10⁴ Å, 5 μm). THF (Fisher, HPLC grade) was used as eluent at a flow rate of 1 mL/min. The number-average (M_n) and weight-average (M_w) molecular weights of PMA samples were determined with PMMA standards purchased American Polymer Standards. As the hydrodynamic volume of PMA is the same as of PMMA, no correction is needed in the determination of M_n .

Typical Procedure for Polymerization Kinetics

The monomer (MA, 1.00 mL, 11.1 mmol), solvent (DMSO, 0.5 mL), initiator (MBP, 5.6 μL, 0.05 mmol), catalyst [12.5 cm of 20 gauge copper (0) wire wrapped around a Teflon-coated stirrer bar], and the ligand (Me_6 -TREN, 1.4 μL, 5 μmol) were added to a 25-mL Schlenk tube in the following order: Cu(0), ligand, initiator, solvent, and monomer. During the freeze-pump-thaw process the stirrer bar was held above the reaction mixture using a small magnet. After six freeze-pump-thaw cycles, the Schlenk tube was filled with nitrogen and placed in an oil bath thermostated at 25 ± 0.1 °C with stirring. The stirrer bar with the catalyst was dropped down to start the polymerization. The side arm of the tube was purged with nitrogen before it was opened for samples to be taken at different intervals throughout the reaction, with an airtight syringe. Samples were dissolved in CDCl₃, and the conversion measured by ¹H NMR spectroscopy. The polymerization mixture was passed through a small basic Al₂O₃ chromatographic column to remove any residual Cu(II)Br₂ deactivator. The solvent and residual monomer were removed under vacuum and the samples dissolved in THF for GPC analysis. The M_n and M_w/M_n values were determined by GPC

with PMMA standards (conversion: 88.7%, $M_n(\text{GPC}) = 20162$, $M_w/M_n = 1.17$).

Computational Techniques

All calculations were performed using Spartan 2008 Quantum Mechanics Program (PC/X86).⁴⁴ Full geometry optimizations and single-point energy calculations of all structures reported were performed via density functional theory (DFT) with the Berke-3-parameter Lee, Yang, Parr hybrid functional (B3LYP) using the 6-31+G* basis set. For compounds with multiple possible conformers, an equilibrium conformer search at the PM3 level (before a conventional geometry optimization) was used to determine the molecular geometry. All geometry optimizations were performed without symmetry constraints. Frequency calculations were performed on all optimized geometries to confirm that they are true minima and to extract thermodynamic parameters. The enthalpy H is corrected for the zero-point vibrational energy. Energy profile calculations for anion radicals and ion-radical pairs were performed with a lower bound bond distance corresponding to the neutral organic halide for 4 Å at intervals of 0.2 Å. All energies were converted from Hartree to kcal mol⁻¹ via the conversion constant of 627.509 kcal mol⁻¹.

Tabulated Values

Homolytic and Heterolytic BDE: The homolytic, E_{homo} , and heterolytic, E_{hetero} , bond dissociation energies were calculated in a standard way according to:

$$E_{\text{homo}} = E_{\text{neutral species}} - E_{\text{radical}} - E_{\text{halogen}} \quad (7)$$

and

$$E_{\text{hetero}} = E_{\text{neutral species}} - E_{\text{radical}} - E_{\text{halide}} \quad (8)$$

E_{RA} is the difference in energy between the neutral species and the ion-radical pair at equilibrium bond distance. It is calculated according to eq 5.

$$E_{\text{RA}} = E_{\text{neutral}} - E_{\text{ion-radical pair}} \quad (9)$$

E_{stab} is the difference in energy between the ion-radical pair and the completely separated radical and halide. It is calculated according to eq 6.

$$E_{\text{stab}} = E_{\text{ion-radical pair}} - E_{\text{neutral}} - E_{\text{anion}} \quad (10)$$

This work was supported by the National Science Foundation (DMR-0548559 and DMR-0520020). The authors gratefully acknowledge P. Roy Vagelos, Chair at Penn.

REFERENCES AND NOTES

- Rosen, B. M.; Percec, V. *Chem Rev* 2009, 109, 5069–5119.
- Rosen, B. M.; Lligadas, G.; Hahn, C.; Percec, V. *J Polym Sci Part A: Polym Chem* 2009, 47, 3940–3948.
- Ouchi, M.; Terashima, T.; Sawamoto, M. *Chem Rev* 2009, 109, 4963–5050.
- Percec, V.; Guliashvili, T.; Ladislaw, J. S.; Wistrand, A.; Stjerndahl, A.; Sienkowska, M. J.; Monteiro, M. J.; Sahoo, S. *J Am Chem Soc* 2006, 128, 14156–14165.
- Potisek, S. L.; Davis, D. A.; Sottos, N. R.; White, S. R.; Moore, J. S. *J Am Chem Soc* 2007, 129, 13808–13809.
- Nguyen, N. H.; Rosen, B. M.; Percec, V. *J Polym Sci Part A: Polym Chem* 2010, 48, 1752–1763.
- Zhai, S.; Wang, B.; Feng, C.; Li, Y.; Dong, Y.; Hu, J.; Lu, G.; Huang, X. *J Polym Sci Part A: Polym Chem* 2009, 48, 647–655.
- Fleischmann, S.; Percec, V. *J Polym Sci Part A: Polym Chem* 2010, 48, 2251–2255.
- Fleischmann, S.; Percec, V. *J Polym Sci Part A: Polym Chem* 2010, 48, 2236–2242.
- Fleischmann, S.; Percec, V. *J Polym Sci Part A: Polym Chem* 2010, 48, 2243–2250.
- Fleischmann, S.; Percec, V. *J Polym Sci Part A: Polym Chem* 2010, 48, 4884–4888.
- Fleischmann, S.; Percec, V. *J Polym Sci Part A: Polym Chem* 2010, 48, 4889–4893.
- Sienkowska, M. J.; Rosen, B. M.; Percec, V. *J Polym Sci Part A: Polym Chem* 2009, 47, 4130–4140.
- Hatano, T.; Rosen, B. M.; Percec, V. *J Polym Sci Part A: Polym Chem* 2009, 48, 164–172.
- Rosen, B. M.; Lligadas, G.; Hahn, C.; Percec, V. *J Polym Sci Part A: Polym Chem* 2009, 47, 3931–3939.
- Whittaker, M. R.; Urbani, C. N.; Monteiro, M. J. *J Polym Sci Part A: Polym Chem* 2008, 46, 6346–6357.
- Lligadas, G.; Percec, V. *J Polym Sci Part A: Polym Chem* 2007, 45, 4684–4695.
- Feng, C.; Shen, Z.; Li, Y.; Gu, L.; Zhang, Y.; Lu, G.; Huang, X. *J Polym Sci Part A: Polym Chem* 2009, 47, 1811–1824.
- Percec, V.; Popov, A. V.; Ramirez-Castillo, E.; Weichold, O. *J Polym Sci Part A: Polym Chem* 2003, 41, 3283–3299.
- Percec, V.; Popov, A. V.; Ramirez-Castillo, E.; Monteiro, M.; Barboiu, B.; Weichold, O.; Asandei, A. D.; Mitchell, C. M. *J Am Chem Soc* 2002, 124, 4940–4941.
- Odian, G. *Principles of Polymerization*; Wiley Interscience: Staten Island, 2004; pp198–349.
- Rosen, B. M.; Percec, V. *J Polym Sci Part A: Polym Chem* 2008, 46, 5663–5697.
- Matyjaszewski, K.; Xia, J. *Chem Rev* 2001, 101, 2921–2990.
- Lligadas, G.; Percec, V. *J Polym Sci Part A: Polym Chem* 2008, 46, 6880–6895.
- Nguyen, N. H.; Rosen, B. M.; Jiang, X.; Fleischmann, S.; Percec, V. *J Polym Sci Part A: Polym Chem* 2009, 47, 5577–5590.
- Nguyen, N. H.; Rosen, B. M.; Lligadas, G.; Percec, V. *Macromolecules* 2009, 42, 2379–2386.
- Jiang, X.; Fleischmann, S.; Nguyen, N. H.; Rosen, B. M.; Percec, V. *J Polym Sci, Part A: Polym Chem* 2009, 47, 5591–5605.
- Ando, T.; Kamigaito, M.; Sawamoto, M. *Tetrahedron* 1997, 53, 15445–15457.
- Matyjaszewski, K.; Wang, J.-L.; Grimaud, T.; Shipp, D. A. *Macromolecules* 1998, 31, 1527–1534.
- Guliashvili, T.; Percec, V. *J Polym Sci Part A: Polym Chem* 2007, 45, 1607–1618.
- Cardinale, A.; Isse, A. A.; Gennaro, A.; Robert, M.; Savéant, J.-M. *J Am Chem Soc* 2002, 124, 13533–13539.
- Nguyen, N. H.; Percec, V. *J Polym Sci Part A: Polym Chem* 2010, 48, 5109–5119.
- Tang, W.; Kwak, Y.; Braunecker, W.; Tsarevsky, N. V.; Coote, M. L.; Matyjaszewski, K. *J Am Chem Soc* 2008, 130, 10702–10713.
- Lligadas, G.; Rosen, B. M.; Monteiro, M. J.; Percec, V. *Macromolecules* 2008, 41, 8360–8364.
- Nguyen, N. H.; Jiang, X.; Fleischmann, S.; Rosen, B. M.; Percec, V. *J Polym Sci Part A: Polym Chem* 2009, 47, 5629–5638.
- Moineau, G.; Minet, M.; Dubois, P.; Teyssie, P.; Senninger, T.; Jerome, R. *Macromolecules* 1998, 32, 27–35.
- Percec, V.; Barboiu, B.; Grigoras, C.; Bera, T. K. *J Am Chem Soc* 2003, 125, 6503–6516.
- Percec, V.; Grigoras, C.; Kim, H. J. *J Polym Sci Part A: Polym Chem* 2004, 42, 505–513.
- Percec, V.; Grigoras, C.; Bera, T. K.; Barboiu, B.; Bissel, P. *J Polym Sci Part A: Polym Chem* 2005, 43, 4894–4906.
- Percec, V.; Bera, T. K.; De, B. B.; Sanai, Y.; Smith, J.; Holerca, M. N.; Barboiu, B.; Grubbs, R. B.; Frechet, J. M. J. *J Org Chem* 2001, 66, 2104–2117.
- Ciampolini, M.; Nardi, N. *Inorg Chem* 1966, 5, 41–44.
- Kavitha, A. A.; Singha, N. K. *Macromolecules*, 43, 3193–3205.
- Sienkowska, M. J.; Percec, V. *J Polym Sci Part A: Polym Chem* 2009, 47, 635–652.
- Shao, Y.; Molnar, L. F.; Jung, Y.; Kussmann, J.; Ochsenfeld, C.; Brown, S. T.; Gilbert, A. T. B.; Slipchenko, L. V.; Levchenko, S. V.; O'Neill, D. P., Jr., R. A. D.; Lochan, R. C.; Wang, T.; Beran, G. J. O.; Besley, N. A.; Herbert, J. M.; Lin, C. Y.; Voorhis, T. V.; Chien, S. H.; Sodt, A.; Steele, R. P.; Rassolov, V. A.; Maslen, P. E.; Korambath, P. P.; Adamson, R. D.; Austin, B.; Baker, J.; Byrd, E. F. C.; Dachsel, H.; Doerksen, R. J.; Dreuw, A.; Dunietz, B. D.; Dutoi, A. D.; Furlani, T. R.; Gwaltney, S. R.; Heyden, A.; Hirata, S.; Hsu, C.-P.; Kedziora, G.; Khalliulin, R. Z.; Klunzinger, P.; Lee, A. M.; Lee, M. S.; Liang, W.; Lotan, I.; Nair, N.; Peters, B.; Proynov, E. I.; Pieniazek, P. A.; Rhee, Y. M.; Ritchie, J.; Rosta, E.; Sherrill, C. D.; Simmonett, A. C.; Subotnik, J. E.; Li, H. L. W.; Zhang, W.; Bell, A. T.; Chakraborty, A. K. *Phys Chem Chem Phys* 2006, 8, 3172–3191.